Journal of Statistical Physics, Vol. 95, Nos. 5/6, 1999

Interfacial Stress, Interfacial Energy, and Phase Equilibria in Binary Alloys

William C. Johnson[1] **and P. W. Voorhees**[2]

Received August 20, 1998

A simple model is presented in order to explore the influence of interfacial stress, interfacial energy, and surface stress on the characteristics of phase equilibria in stressed, two-phase binary alloys. Two different system geometries are employed: concentric spheres and thin plates. The conditions for thermodynamic equilibrium are solved and equations of state for each geometry are obtained in terms of the phase fraction, alloy composition, system dimension, and several dimensionless materials parameters. Elastic stress introduces new equilibrium states that are further modified by the interfacial quantities. Those conditions for which interfacial quantities can induce significant changes in the equilibrium phase fraction and phase compositions are identified.

KEY WORDS: Phase equilibrium; interfacial stress; surface stress; elastic stress.

1. INTRODUCTION

John Cahn has had a strong influence on our research, particularly in the areas of the thermodynamics of crystalline solids and the role of elastic stress in solid-state phase transformations. Two areas to which John has introduced us and which we have found particularly intriguing, are the effect of coherency stress on phase equilibria in crystalline solids[1–3] and the influence of capillarity on the thermodynamics of crystals.[4, 5] His paper with F. Larché in 1984 on *A Simple Model for Coherent Equilibrium*,[2] in particular, raised tantalizing questions about the rules governing phase equilibria in stressed, coherent systems. In this work, based on a simple model for

[1] Department of Materials Science and Engineering, University of Virginia, Charlottesville, Virginia 22903-2442.

[2] Department of Materials Science and Engineering, Northwestern University, Evanston, Illinois 60208.

0022-4715/99/0600-1281$16.00/0

the elastic and chemical energy of a two-phase system, Cahn and Larché argued that a number of general theorems of thermodynamics derived for fluid systems were not applicable to multiphase crystals with coherent interfaces. For example, tie lines drawn in a temperature-composition phase diagram did not necessarily end on phase boundaries and were a function of the alloy (bulk) composition. In addition, the applicability of Gibbs' phase rule to coherent systems was called into question. These results, along with John's encouragement, motivated our own investigation of phase equilibria in coherent systems[6–13] and sparked the research of several other investigators.[14–20]

In the early 1980's, Cahn also elucidated some simple models exploring the effect of interfacial energy, surface stress, and interfacial stress on the phase equilibria of small particles embedded in fluid or crystalline matrices.[4, 5] Owing to the difference between interfacial stress and interfacial energy in crystalline solids, some of the well-accepted, fundamental consequences of capillarity were shown to be modified when one of the phases was a crystal. For example, when substitutional atoms are added to the system, work is done against the interfacial energy, while work is done against the interfacial stress when the interface is deformed. We used these results to explore interfacial equilibrium during a simple diffusional phase transformation in a stressed crystal.[21]

With the current prevalence of nanostructured materials and thin-film devices, the influence of interfacial stress and interfacial energy on phase equilibria and phase stability in multicomponent systems becomes of practical concern. For crystals with dimensions on the order ten to hundreds of nanometers, interfacial stresses can generate bulk stresses in single-phase materials that would be expected to shift significantly compositions and chemical potentials from the values they would have in large systems. At such dimensions, the interfacial energy can become a non-negligible fraction of the system energy. The coupling of elastic stress and interfacial effects results in many cases in which a matrix or substrate stabilizes a phase not found on the phase diagram.[22] The effect of interfacial stress on the relative stability of phases in a two-phase systems remains largely unexplored.

In this paper, we explore the effect of interfacial stress, surface stress, and interfacial energy on the equilibrium phase compositions, phase fraction, and phase stability of a two-phase, coherent binary alloy system. We use the bulk and interfacial conditions for thermodynamic equilibrium to obtain a set of equations for the phase compositions and phase fraction. This guarantees that the appropriate free energy of the system is an extremum and, thereby, identifies both energy maxima (unstable states) and energy minima (stable or metastable states). The shift in equilibrium

phase compositions from those of the unstressed equilibrium state are linearized to obtain an equation of state for the stressed system in terms of the phase fraction, alloy composition, system dimension, and various materials parameters. The elastic fields experienced by each phase are affected by the system geometry and the interfacial conditions for thermodynamic equilibrium depend on the local curvature of the interface. These conditions suggest that, unlike fluid systems, the system geometry and spatial distribution of the phases will strongly affect equilibrium. Consequently, we limit our analysis to two, experimentally observed geometries that are relevant to nanoscale materials and which guarantee that all bulk and interfacial equilibrium conditions can be satisfied simultaneously. The system geometries employed are two concentric spheres with isotropic properties and a thin-film system of parallel layers or plates with cubic symmetry. The equations of state for the two system geometries including capillarity effects are presented in the next two sections. These results are then compared with bulk equilibrium phenomena in the following section.

2. EQUILIBRIUM CONDITIONS

2.1. Mechanical Equilibrium

We consider phase equilibria in a two-phase ($\alpha - \beta$) crystalline solid. Each phase is assumed to be a binary substitutional alloy of components A and B. The phases can differ in their thermodynamic properties including composition, elastic constants, and molar volumes. Crystal lattice parameters and elastic constants are assumed independent of composition. All interfacial and surface quantities are assumed isotropic and independent of composition and deformation.

The coherency constraint requires that a continuity of the lattice planes be maintained at all times across the $\alpha - \beta$ interface. This implies that there is a lattice common to both phases to which the deformation of each phase can be referred. Our treatment of coherent phase equilibria consists of isothermally arranging a given number of A and B atoms (determined by the mole fraction of the bulk alloy) on this common lattice in one of the two *predetermined* geometries. The atoms are limited to either the α- or β-phases. Other geometries or spatial arrangements of the phases could exist which satisfy the thermodynamic equilibrium conditions, such as concentric cylinders, but these two simple models serve to illustrate the influence that interfacial properties might have on the characteristics of phase equilibria in nanoscale systems.

For the thin-film and concentric sphere geometries, the reference state for measuring strain, $\mathbf{E}$, is taken to be the unstressed α-phase. If the stress-

free β-phase has a different lattice parameter than that of the stress-free α-phase, the β phase will be stressed when deformed into the reference state. Let $\mathbf{E}^T$ be the strain required to transform the stress-free β-phase into the reference state as measured with respect to the reference state (the misfit strain). The stress state of each phase, $\mathbf{T}$, is then given by:

$$\mathbf{T}^\alpha = \mathbf{C}^\alpha \cdot \mathbf{E} \qquad \text{and} \qquad \mathbf{T}^\beta = \mathbf{C}^\beta \cdot (\mathbf{E} - \mathbf{E}^T) \tag{1}$$

where $\mathbf{C}$ is the elastic constants tensor for the indicated phase. As we will consider isotropic and cubic crystals, the misfit strain is isotropic and dilatational, and can be expressed in terms of the misfit strain, ε, as $\mathbf{E}^T = \varepsilon\mathbf{1}$, where $\mathbf{1}$ is the unit tensor. Mechanical equilibrium in each phase requires:

$$\nabla \cdot \mathbf{T}^\alpha = \mathbf{0} \qquad \text{and} \qquad \nabla \cdot \mathbf{T}^\beta = \mathbf{0} \tag{2}$$

The coherency constraint requires the continuity of displacement, $\mathbf{u}$, at the $\alpha - \beta$ interface:

$$\mathbf{u}^\alpha = \mathbf{u}^\beta \tag{3}$$

Mechanical force balance at the coherent $\alpha - \beta$ interface requires:

$$\mathbf{T}^\alpha \cdot \hat{\mathbf{n}}^\alpha + \mathbf{T}^\beta \cdot \hat{\mathbf{n}}^\beta + \hat{f}_I \kappa^\beta \hat{\mathbf{n}}^\beta = \mathbf{0} \tag{4}$$

where $\hat{\mathbf{n}}$ is the outward pointing unit normal to the indicated phase, $\hat{\mathbf{f}}_I = \hat{f}_I \mathbf{1}$ is the isotropic *interfacial* stress acting at the $\alpha - \beta$ interface, and κ^β is the mean curvature measured with respect to the β-phase. Mechanical equilibrium at a free surface of α-crystal is given by a similar force balance:

$$\mathbf{T}^\alpha \cdot \hat{\mathbf{n}}^\alpha = -(P_{ext} + \hat{f}_s \kappa^\alpha)\, \hat{\mathbf{n}}^\alpha \tag{5}$$

where P_{ext} is the external pressure acting on the crystal and $\hat{f}_s$ is the isotropic *surface* stress ($\hat{\mathbf{f}}_s = \hat{f}_s \mathbf{1}$). Our assumption of the composition independence of the elastic constants, misfit strain and lattice parameter of each phase allows the mechanical field equations to be decoupled from the other equilibrium conditions. The elastic fields associated with each system geometry are calculated in Appendices I and II in terms of the phase fraction of each phase.

2.2. Thermodynamic Equilibrium

In order to completely specify the thermodynamic state of this isothermal two-phase system, one must determine the compositions of each phase

and the phase fraction. These three unknowns are determined through a solution to the two nonlinear equations governing thermodynamic equilibrium and one equation for mass conservation, once the elastic field has been determined.

The first of the three equations necessary to ensure equilibrium (an energy extremum) is given by the requirement that the diffusion potential, M_{BA}, be uniform within each phase and, in particular, continuous at the $\alpha-\beta$ interface. As the elastic constants and molar volumes are assumed independent of composition, the diffusion potential depends on the local composition only and not on the stress state. Under these conditions, the diffusion potential can be expressed simply as:[23]

$$M_{BA}=\mu_B(C)-\mu_A(C) \tag{6}$$

where μ_B is the usual (stress-free) chemical potential of component B, and C is the mole fraction (composition) of component B. Chemical equilibrium between phases requires:[23]

$$M^{\alpha}_{BA}(C^{\alpha})=M^{\beta}_{BA}(C^{\beta}) \tag{7}$$

or, using Eq. (6),

$$\mu^{\alpha}_{B}(C^{\alpha})-\mu^{\alpha}_{A}(C^{\alpha})=\mu^{\beta}_{B}(C^{\beta})-\mu^{\beta}_{A}(C^{\beta}) \tag{8}$$

The second equation is given by a condition involving the jump in the free energy densities, Ξ_v, evaluated at the planar $\alpha-\beta$ interface:[24, 25]

$$\Xi^{\beta}_{v}-\Xi^{\alpha}_{v}=-\kappa^{\beta}\sigma+[(\hat{\mathbf{F}}^{T}\cdot\hat{\mathbf{f}}_I)\cdot\bar{\nabla}_{\Sigma}]\cdot\hat{\mathbf{n}} \tag{9}$$

where σ is the deformation-dependent (isotropic) interfacial free energy density, $\hat{\mathbf{F}}^T$ is the transpose of the interfacial deformation gradient, $\bar{\nabla}_{\Sigma}$ is the surface divergence operator, and the free energy density Ξ_v is defined by:

$$\Xi_v=e_v-\theta\eta_v-M_{BA}\rho_B-(\mathbf{T}_R\cdot\hat{\mathbf{n}})\cdot(\mathbf{F}\cdot\hat{\mathbf{n}}) \tag{10}$$

where e_v is the internal energy density, θ is the absolute temperature, η_v is the entropy density, $\mathbf{T}_R$ is the first Piola–Kirchoff stress tensor, and $\mathbf{F}$ is the deformation gradient tensor. Invoking linear elasticity and under the assumptions given previously, Eq. (9) becomes:[24]

$$\rho_o[\mu^{\beta}_{A}(C^{\beta})-\mu^{\alpha}_{A}(C^{\alpha})]+\kappa^{\beta}\sigma+E_{el}=0 \tag{11}$$

where

$$E_{el}=\tfrac{1}{2}\mathbf{T}^{\beta}:(\mathbf{E}^{\beta}-\mathbf{E}^{T})-\tfrac{1}{2}\mathbf{T}^{\alpha}:\ \mathbf{E}^{\alpha}+\mathbf{T}^{\beta}:(\mathbf{E}^{\alpha}-\mathbf{E}^{\beta})+\kappa^{\beta}\hat{f}_I\hat{\mathbf{n}}\cdot(\mathbf{E}^{\alpha}-\mathbf{E}^{\beta})\cdot\hat{\mathbf{n}} \tag{12}$$

The notation $\mathbf{T}:\ \mathbf{E} = T_{ij}E_{ij}$ represents the scalar product of the stress and strain tensors and summation over repeated indices extends from 1 to 3.

Finally, the third equation is obtained from mass conservation which can be expressed as:

$$(1-z)\ C^{\alpha} + zC^{\beta} = C_o \tag{13}$$

where C_o is the overall (bulk) alloy composition and z is the phase fraction of β.

The set of Eqs. (8), (11), and (13) are nonlinear and, in general, must be solved numerically. However, if the departures of the equilibrium phase compositions in the stressed state from those of the stress-free state are small, then the chemical potentials can be written to first order in terms of the shift of composition from the stress-free equilibrium compositions, C_o^{α} and C_o^{β}. As shown in Appendix III, the condition on chemical equilibrium, Eq. (8), is approximated as:

$$f_{cc}^{\alpha}\,\Delta C^{\alpha} = f_{cc}^{\beta}\,\Delta C^{\beta} \tag{14}$$

where $\Delta C^{\alpha} = C^{\alpha} - C_o^{\alpha}$, $\Delta C^{\beta} = C^{\beta} - C_o^{\beta}$ and f_{cc} is the second derivative with respect to composition of the Helmholtz free energy per atom for the designated phase evaluated at the stress-free equilibrium compositions Likewise, Eq. (11) can be approximated as:

$$\rho_o C_o^{\alpha} f_{cc}^{\alpha}\,\Delta C^{\alpha} - \rho_o C_o^{\beta} f_{cc}^{\beta}\,\Delta C^{\beta} + \kappa^{\beta}\sigma + E_{el} = 0 \tag{15}$$

where ρ_o is the number of atoms per unit volume. Solving Eqs. (13)–(15) for ΔC^{α}, ΔC^{β} and z gives:

$$\Delta C^{\alpha} = \frac{\kappa^{\beta}\sigma + E_{el}}{\rho_o (C_o^{\beta} - C_o^{\alpha})\, f_{cc}^{\alpha}} \tag{16}$$

$$\Delta C^{\beta} = \frac{\kappa^{\beta}\sigma + E_{el}}{\rho_o (C_o^{\beta} - C_o^{\alpha})\, f_{cc}^{\beta}} \tag{17}$$

and

$$\frac{f_{cc}^{\beta}[(C_o - C_o^{\alpha}) - (C_o^{\beta} - C_o^{\alpha})\, z]}{[f_{cc}^{\beta} + (f_{cc}^{\alpha} - f_{cc}^{\beta})\, z]} = \frac{\kappa^{\beta}\sigma + E_{el}}{\rho_o (C_o^{\beta} - C_o^{\alpha})\, f_{cc}^{\alpha}} \tag{18}$$

In order to determine the phase compositions and phase fraction, it is necessary to calculate the stresses and strains at the interface. Since the composition is not coupled directly to the stresses and strains, due to the assumed independence of the lattice parameters and elastic constants on

composition, we can use these three equations to determine the equilibrium compositions and phase fraction for both the thin film and concentric sphere arrangement of the phases.

Finally, we find it convenient to introduce scaled compositions for the α-phase (Γ_α), β-phase (Γ_β), and alloy (Γ_o) as:

$$\Gamma_\alpha = -1 + 2(C^\alpha - C_o^\alpha)/(C_o^\beta - C_o^\alpha) \tag{19}$$

$$\Gamma_\beta = 1 + 2(C^\beta - C_o^\beta)/(C_o^\beta - C_o^\alpha) \tag{20}$$

and

$$\Gamma_o = -1 + 2(C_o - C_o^\alpha)/(C_o^\beta - C_o^\alpha) \tag{21}$$

In the absence of elastic or curvature effects, the scaled phase compositions at equilibrium are independent of the alloy composition, Γ_o, and are given by $\Gamma_\alpha = -1$ and $\Gamma_\beta = 1$. The two-phase field exists for $-1 < \Gamma_o < 1$. We express the difference in the curvature of the free energy densities in terms of the nondimensional parameter ζ as:

$$\zeta = (f_{cc}^\alpha - f_{cc}^\beta)/f_{cc}^\beta \tag{22}$$

Substituting Eqs. (21) and (22) into Eq. (18), gives:

$$\frac{(\Gamma_o + 1 - 2z)}{(1 + \zeta z)} = \frac{2(\kappa^\beta \sigma + E_{el})}{\rho_o (C_o^\beta - C_o^\alpha)^2 f_{cc}^\alpha} \tag{23}$$

For the geometries we are examining, E_{el} can be expressed in terms of the phase fraction z and an overall system dimension. This will allow Eq. (23) to be used as an equation of state for calculating the equilibrium phase fraction z as a function of the imposed conditions, system size, and materials parameters. Likewise, the scaled phase compositions Γ_α and Γ_β can be expressed in terms of the equilibrium phase fraction by combining the mass conservation condition, Eq. (13), and the approximation, Eq. (15), with Eqs. (19) and (20) to yield:

$$\Gamma_\alpha = -1 + \frac{(\Gamma_o + 1 - 2z)}{(1 + \zeta z)} \tag{24}$$

and

$$\Gamma_\beta = 1 + \frac{(\zeta + 1)(\Gamma_o + 1 - 2z)}{(1 + \zeta z)} \tag{25}$$

In the following sections we obtain the equation of state for each of the system geometries. We note that, in the absence of elastic effects and interfacial curvature, Eq. (23) reduces to a single solution for the phase fraction:

$$z = (\Gamma_o + 1)/2 \tag{26}$$

The corresponding scaled equilibrium phase compositions, $\Gamma_\alpha = -1$ and $\Gamma_\beta = 1$, are constant and independent of the alloy composition when Eq. (26) is realized.

3. THIN-FILM GEOMETRY

In this section, we derive equations for the equilibrium phase compositions and phase fraction and an equation of state for the $\alpha - \beta$ system when the phases are arrayed as thin parallel plates, as depicted in Fig. 1. Two cases are considered. In the first, the misfit strain is assumed to vanish. This allows the effect of the interfacial stress on phase equilibrium to be assessed directly. In the second case, the misfit strain is included.

The crystallographic axes of each cubic phase are assumed to be aligned with the coordinate axes and the $\alpha - \beta$ interfaces are taken parallel to the $x_1 - x_2$ plane. The thickness of the phases are l_α and l_β, respectively, with a repeat distance of $l_\alpha + l_\beta = L$. The isotropic interfacial stress, which exerts a mechanical force per unit length of interface, is given by $\hat{f}_I$. The external stress T_{ap} is applied along the edge of the plates equally in the x_1 and x_2-directions, while no external stresses are applied in the x_3-direction.

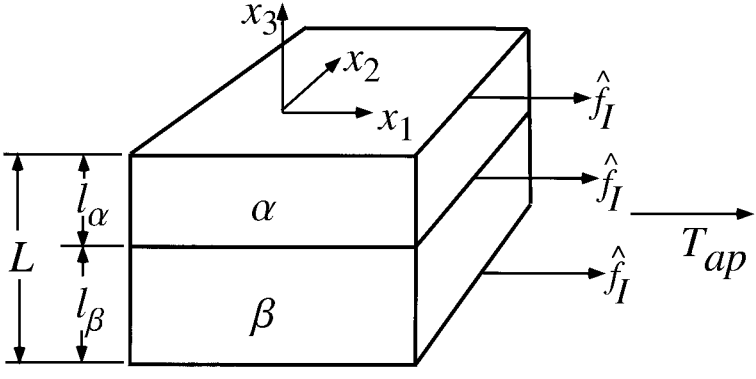

Fig. 1. For the thin-film geometry, the crystallographic axes of the cubic phases are aligned with the coordinate axes. The interfacial stress, $\hat{f}_I$, exerts a force per unit length of $\alpha - \beta$ interface in the x_1 and x_2 directions along the edge of the film. This interfacial stress is balanced by the uniform stress in each phase and the applied stress, T_{ap}, and is the only means by which the interfacial stress affects phase equilibria in this geometry.

The assumptions used in this model allow the elastic field of the phases to be determined as a function of the phase fraction of β phase, $z = l_\beta/L$, the repeat distance L, the interfacial stress, and the elastic constants of the phases. If bending of the plates is prohibited, as would be expected for an array of plates, the interfacial curvature is zero and the $\kappa^\beta\sigma$ and $\kappa^\beta\hat{f}_I$ terms vanish on the $\alpha-\beta$ interface. The stresses, strains and strain energy density for both phases are calculated in Appendix I. Additionally, the elastic state and, hence, thermodynamic state within each phase is uniform.

3.1. No Misfit Strain

When the misfit strain vanishes, $\varepsilon = 0$, the elastic field is engendered by the applied stress, T_{ap}, and interfacial stress, $\hat{f}_I$. Setting $\varepsilon = 0$ in Eqs. (79) and (80) of Appendix I yields:

$$E_{el} = \frac{\delta_p[\,T_{ap} - 2\hat{f}_I/L\,]^2}{Y_\alpha(1+\delta_p z)^2} \tag{27}$$

where Y is the planar elastic modulus given by Eq. (77), and δ_p is a measure of the difference in the planar elastic moduli between phases:

$$\delta_p = (\,Y_\beta - Y_\alpha)/Y_\alpha \tag{28}$$

Substituting Eq. (27) into Eq. (23), we obtain the equation of state for the planar system without misfit strain:

$$(\Gamma_o + 1 - 2z) = \frac{\delta_p \Lambda_m(1+\zeta z)}{(1+\delta_p z)^2} \tag{29}$$

where we define the dimensionless stress parameter, Λ_m, as:

$$\Lambda_m = \frac{2[\,T_{ap} - 2\hat{f}_I/L\,]^2}{Y_\alpha \rho_o f^\alpha_{cc}(C^\beta_o - C^\alpha_o)^2} \tag{30}$$

Values of z which satisfy Eq. (29) with $0 \leqslant z \leqslant 1$ give phase fractions which satisfy all thermodynamic equilibrium conditions. The phase compositions corresponding to the phase fraction are obtained from Eqs. (24) and (25). Nonzero values of Λ_m change the equation of state from a linear polynomial to a cubic polynomial in z. This condition allows for multiple equilibrium states for a given alloy composition and applied stress.

Case: $\epsilon = 0$ and $|\Lambda_m| \ll 1$. In many cases, but not all, we expect $|\Lambda_m| \ll 1$.[3] If so, we can examine the effect of the interfacial stress on the equilibrium phase fraction and compositions in the case of no misfit strain by writing:

$$z = z_o + z_m \Lambda_m + O(\Lambda_m^2) \tag{31}$$

Substituting Eq. (31) into Eq. (29) and collecting terms of like order in Λ_m gives $z_o = (\Gamma_o + 1)/2$ and:

$$z \approx (\Gamma_o + 1)/2 - \frac{\delta_p[2 + \zeta(\Gamma_o + 1)]}{[2 + \delta_p(\Gamma_o + 1)]^2} \Lambda_m \qquad (\varepsilon = 0) \tag{32}$$

The corresponding equilibrium phase compositions are obtained by substituting Eq. (32) into Eqs. (24) and (25):

$$\Gamma_\alpha \approx -1 + \frac{4\delta_p \Lambda_m}{[2 + \delta_p(\Gamma_o + 1)]^2} \qquad (\varepsilon = 0) \tag{33}$$

and

$$\Gamma_\beta \approx 1 + \frac{4(1 + \zeta)\, \delta_p \Lambda_m}{[2 + \delta_p(\Gamma_o + 1)]^2} \qquad (\varepsilon = 0) \tag{34}$$

3.2. Misfit Strain

When the misfit strain is nonzeros the elastic term, E_{el}, becomes:

$$E_{el} = \frac{Y_\alpha \varepsilon^2}{(1 + \delta_p z)^2} [\, -\delta_p(1 + \delta_p)\, z^2 - 2(1 + \delta_p)\, z + (1 + \delta_p)(1 - 2\tau_{11}^o) + \delta_p(\tau_{11}^o)^2] \tag{35}$$

where we define:

$$\tau_{11}^o = T_{11}^o / \varepsilon Y_\alpha = [\, T_{ap} - 2\hat{f}_I / L] / \varepsilon Y_\alpha \tag{36}$$

τ_{11}^o is the nondimensional measure of the effective stress (T_{11}^o) acting along the edge of the thin film. It depends on the thickness of the system L as well as the applied stress T_{ap}. Substituting Eq. (35) into Eq. (23) and defining the scaled elastic parameter, Λ_p, as:

$$\Lambda_p = \frac{2\varepsilon^2 Y_\alpha}{\rho_o f_{cc}^\alpha (C_o^\beta - C_o^\alpha)^2} \tag{37}$$

[3] For example, near a congruent point, we expect $|\Lambda_m|$ to be large.

yields the following cubic polynomial equation for the equilibrium phase fraction z:

$$\frac{(\Gamma_o + 1 - 2z)}{(1+\zeta z)} = \frac{\Lambda_p}{(1+\delta_p z)^2}\left[-\delta_p(1+\delta_p)\, z^2 - 2(1+\delta_p)\, z + (1+\delta_p)(1-2\tau_{11}^o) + \delta_p(\tau_{11}^o)^2\right] \quad (38)$$

We refer to Eq. (38) as the equation of state for the misfitting thin-film system. Phase fractions (values of z) which satisfy Eq. (29) and the constraint $0 \leqslant z \leqslant 1$ satisfy all thermodynamic equilibrium conditions. However, the system could be either stable or unstable with respect to small changes in the phase fraction. The corresponding phase compositions are obtained from Eqs. (24) and (25).

Case: $\tau_{11}^o = 0$ and $|\Lambda_p| \ll 1$. The effect of the misfit strain on the equilibrium phase fraction and phase compositions, as compared to the stress-free case, can be estimated when the scaled elastic parameter is small, $\Lambda_p \ll 1$. Setting $\tau_{11}^o = 0$ for consistency, we assume $z = z_o + z_p \Lambda_p + O(\Lambda_p^2)$ and substitute this expression into Eq. (38). Keeping terms to first order in Λ_p gives:

$$z \approx \frac{(\Gamma_o + 1)}{2} + z_p \Lambda_p \qquad (\tau_{11}^o = 0) \quad (39)$$

where:

$$z_p = \frac{[2+\zeta(\Gamma_o+1)]}{4[2+\delta_p(\Gamma_o+1)]^2}\left[\delta_p(1+\delta_p)(\Gamma_o+1)^2 + 4(1+\delta_p)\,\Gamma_o\right] \qquad (\tau_{11}^o = 0) \quad (40)$$

The scaled phase compositions are approximated by:

$$\Gamma_\alpha \approx -1 - \frac{4 z_p \Lambda_p}{[2+\zeta(\Gamma_o+1)]} \qquad (\tau_{11}^o = 0) \quad (41)$$

and

$$\Gamma_\beta \approx 1 - \frac{4 z_p (1+\zeta)\, \Lambda_p}{[2+\zeta(\Gamma_o+1)]} \qquad (\tau_{11}^o = 0) \quad (42)$$

Equations (39)–(42) express the phase fraction and compositions for the stressed state as a perturbation about the equilibrium state of the

unstressed system. It does not account for possible additional solutions that are introduced owing to the elasticity.[6]

Case: $|\tau_{11}^o| \ll 1$ and $\delta_p = 0$. We can also approximate the effect of the interfacial stress $\hat{f}_I$ and system dimension L on the equilibrium phase fraction and compositions using a perturbation analysis similar to that just given. In order to avoid unnecessary complexity, these effects are best illustrated by assuming elastic homogeneity; i.e., by setting $\delta_p = 0$. If $|\tau_{11}^o| \ll 1$, then we approximate:

$$z = z_o + z_t \tau_{11}^o + O((\tau_{11}^o)^2) \tag{43}$$

Substituting Eq. (43) into Eq. (38) and grouping terms of like order in τ_{11}^o, we find z_o is a solution of the quadratic equation:

$$2\zeta \Lambda_p z_o^2 + [(2-\zeta)\,\Lambda_p - 2]\, z_o + \Gamma_o + 1 - \Lambda_p = 0 \qquad (\delta_p = 0) \tag{44}$$

and that z_t depends on the value of z_o according to:

$$z_t = \frac{2\Lambda_p(1+\zeta z_o)}{[2-\Lambda_p - 2\Lambda_p(1+\zeta)\, z_o]} \qquad (\delta_p = 0) \tag{45}$$

The equilibrium phase compositions are then determined from Eqs. (24) and (25). The possible existence of two solutions for Eq. (44) indicates that, for $\delta_p = 0$, there exists two possible equilibrium states. Only one of these states will be stable with respect to variations in the phase fraction.[6]

Case: $\delta_p = 0$ and $\zeta = 0$. For the case of elastic homogeneity ($\delta_p = 0$) and when the curvatures of the free energy densities are the same ($\zeta = 0$), the equation of state is linear and only one equilibrium state is possible. The equilibrium phase fraction is given by:

$$z = \frac{\Gamma_o + 1 - \Lambda_p + 2\Lambda_p \tau_{11}^o}{2(1-\Lambda_p)} \qquad (\delta_p = \zeta = 0) \tag{46}$$

The corresponding scaled phase compositions are:

$$\Gamma_\alpha = -1 - \frac{\Lambda_p(\Gamma_o + 2\tau_{11}^o)}{(1-\Lambda_p)} \qquad (\delta_p = \zeta = 0) \tag{47}$$

and

$$\Gamma_\beta = 1 - \frac{\Lambda_p(\Gamma_o + 2\tau_{11}^o)}{(1-\Lambda_p)} \qquad (\delta_p = \zeta = 0) \tag{48}$$

4. SPHERICAL PARTICLES

4.1. Governing Equations

A schematic diagram of the spherical system is shown in Fig. 2. The β-phase has a radius of R^β and is centered at the origin. The α-phase has an outer radius of R^α and the phase fraction of β is expressed as $z = (R^\beta/R^\alpha)^3$. The elastic fields can be expressed as a function of z and the outer radius R^α. The position-dependent elastic fields for the phases are determined in Appendix II. The elastic energy densities evaluated at the interface yield to first order in $\hat{f}_I$:

$$E_{el} = \frac{-9\varepsilon^2 K^\beta[\delta_s z^2 + 2z - 1] + 9\Gamma P[2\varepsilon K^\beta + \Gamma^* K^\alpha \delta_s P]}{2\Gamma^*(1+\delta_s z)^2} + \frac{6\Gamma \hat{f}_I z}{\Gamma^* R^\beta (1+\delta_s z)^2}\left[P\delta_s + \frac{K_\beta \varepsilon}{K_\alpha \Gamma^*}\right] \tag{49}$$

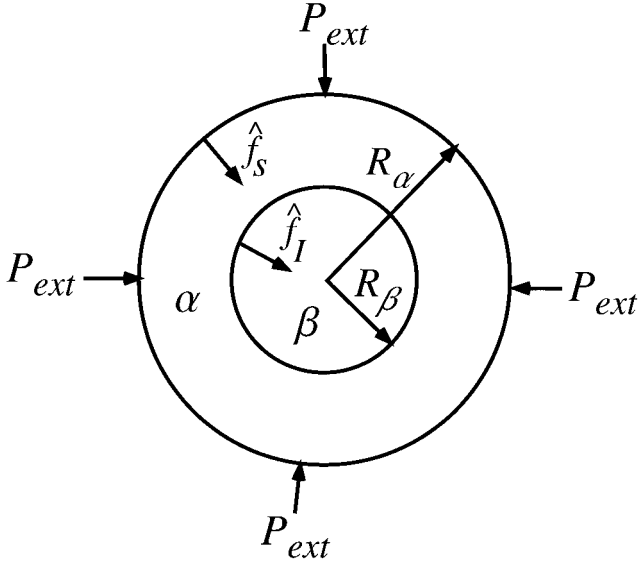

Fig. 2. All materials properties are assumed to be isotropic for the concentric sphere geometry and the inner phase is taken as β with radius R^β. The interfacial stress $\hat{f}_I$ exerts a radial force at $r = R^\beta$ and the surface stress $\hat{f}_s$ and external pressure P_{ext} exert a radial force at $r = R^\alpha$.

where K and μ are the bulk and shear moduli, respectively, of the indicated phase, and:

$$P = (P_{ext} + 2\hat{f}_s/R^\alpha)/3K^\alpha \tag{50}$$

$$\delta_s = (K^\beta - K^\alpha)/K^\alpha \Gamma^* \tag{51}$$

$$\Gamma = (3K^\alpha + 4\mu^\alpha)/4\mu^\alpha \tag{52}$$

and

$$\Gamma^* = (3K^\beta + 4\mu^\alpha)/4\mu^\alpha \tag{53}$$

If Eq. (49) is substituted into Eq. (23) an equation of state for the spherically symmetric system can be obtained. This is a complicated expression in z and R^α that needs to be solved numerically and requires an expression for the elastic component of the interfacial energy density σ. The presence of an interfacial stress leads to the last term Eq. (49), the remaining terms are identical to those found previously when $R^\alpha \to \infty$.[6] Note that the interfacial stress term that arises from the bulk elastic fields evaluated at the interface is proportional to z/R^β.

Since the interfacial stress $\hat{f}_I$ is assumed constant, the interfacial energy is given by:

$$\sigma = \sigma_o + \hat{f}_I(E^\alpha_{\theta\theta} + E^\alpha_{\phi\phi}) \tag{54}$$

where σ_o is the interfacial energy density in the absence of interfacial deformation. The strain components $E^\alpha_{\theta\theta} = E^\alpha_{\phi\phi}$ are given in Appendix II. If we neglect the dependence of σ on interfacial curvature, Eq. (54) simplifies to:

$$\sigma = \sigma_o + \frac{6\varepsilon\hat{f}_I K^\beta(3K^\alpha + 4\mu^\alpha z)}{[3K^\alpha(3K^\beta + 4\mu^\alpha) + 12\mu^\alpha(K^\beta - K^\alpha)\, z]} \tag{55}$$

The dependence of the interfacial energy on the phase fraction arises because the elastic fields depend on the phase fraction.

The thermodynamics used to obtain the equation of state is a condition for an energy extremum. Thus, the equation of state should yield an expression for the critical radius of nucleation R^*_β (an energy maximum). Setting $z = 0$ and $P = 0$ in Eqs. (49) and (55), and using Eq. (23) yields:

$$R^*_\beta = \frac{2\sigma_o + 12K^\beta f\varepsilon^T/(3K^\beta + 4\mu^\alpha)}{\Delta F_c - 18\varepsilon^2\mu^\alpha K^\beta/(3K^\beta + 4\mu^\alpha)} \tag{56}$$

where ΔF_c is the change in Helmholtz free energy per unit volume in the limit of small supersaturation:

$$\Delta F_c = \rho_o (C_o - C_o^\alpha)(C_o^\beta - C_o^\alpha) f_{cc}^\alpha \tag{57}$$

This agrees with the expression for the critical radius for nucleation found previously by Cahn and Larche.[5] The expression for ΔF_c is obtained only in the small supersaturation limit due to the linearization of the chemical potentials shown in Appendix III. The interfacial stress terms shown in Eq. (56) are due solely to the dependence of the interfacial energy on interfacial stress, since the surface stress terms appearing in E_{el} disappear in the limit $z = 0$.

The equation of state is quite complicated in the most general case and, consequently, it is necessary to resort to a numerical method to determine the effects of interfacial and surface stress on phase equilibrium. However, in the limit $\delta_s = 0$, the terms involving $\hat{f}_I$ in both Eq. (49) and Eq. (55) are linear in z. Thus, in the limit that the elastic constants of the particle and matrix are identical, the interfacial stress does not alter the order of the equation of state. Both the terms involving the misfit and interfacial stress yield quantities that are linear in z. Thus the presence of an interfacial stress does not alter qualitatively the results found previously in the absence of a surface stress, but will certainly change the results quantitatively.

4.2. Equations of State

Case: $\delta_s = 0$ and $P_{ext} = 0$. A tractable equation of state that indicates the effect of capillarity and stress on phase equilibria in the spherical particles can be obtained by assuming the elastic constants of the two phases to be equal, $\delta_s = 0$, and that there is no external pressure acting on the system, $P_{ext} = 0$.

As for the thin-film case, we define a nondimensional stress parameter Λ_s as:

$$\Lambda_s = \frac{9K^\alpha \varepsilon^2}{\Gamma \rho_o (C_o^\beta - C_o^\alpha)^2 f_{cc}^\alpha} \tag{58}$$

In addition, a quantity related to size of the system can be given in terms of the reciprocal of R^α as:

$$\tau = \frac{3\varepsilon \hat{f}_s}{\rho_o (C_o^\beta - C_o^\alpha)^2 f_{cc}^\alpha R^\alpha} \tag{59}$$

F is defined as the ratio of the interfacial and surface stresses:

$$F = \frac{5\hat{f}_I}{3\gamma\hat{f}_s} \tag{60}$$

and Σ is a nondimensional interfacial term:

$$\Sigma = \frac{\sigma_o}{3\varepsilon\hat{f}_s} - \frac{K^\alpha \hat{f}_I}{(3K^\alpha + 4\mu^\alpha)\,\hat{f}_s} \tag{61}$$

Substituting the expressions for E_{el} and σ into Eq. (23), using the nondimensional parameters defined by Eqs. (58)–(60) and setting $P_{ext} = \delta_s = 0$ gives the following equation of state for the spherical system:

$$\frac{(\Gamma_o + 1 - 2z)}{(1+\zeta z)} = \Lambda_s(1-2z) + \tau[1 + \Sigma z^{-1/3} + Fz^{2/3}] \qquad (\delta_s = 0) \tag{62}$$

Values of the phase fraction z which satisfy Eq. (62) guarantee the conditions for thermodynamic equilibrium are satisfied for the two-phase system when the phases are arrayed in the spherical geometry. Each solution (value of z) will have a corresponding equilibrium phase composition given by Eqs. (24) and (25). These solutions can be stable or unstable.

Case: $\delta_s = 0$, $\zeta = 0$, and $P_{ext} = 0$. If the curvatures of the free energies are equal, $\zeta = 0$, and Eq. (62) simplifies to:

$$2(1-\Lambda_s)\,z^{4/3} + F\tau z + (\Lambda_s - \Gamma_o - 1 + \tau)\,z^{1/3} + \Sigma\tau = 0 \qquad (\delta_s = \zeta = 0) \tag{63}$$

The effect of the system size on the equilibrium phase fraction and phase compositions is determined by the parameter τ, which is inversely proportional to the system radius. We can estimate the magnitude of the capillarity effect by using the equation of state for a system with $\delta_s = 0$ and $\zeta = 0$, Eq. (63), and perturbing about $\tau = 0$. Let:

$$z = z_o + z_s\tau + O(\tau^2) \tag{64}$$

Substituting Eq. (64) into Eq. (63) and collecting like terms yields:

$$z_o = \frac{(\Gamma_o + 1 - \Lambda_s)}{2(1-\Lambda_s)} \qquad (\delta_s = \zeta = 0) \tag{65}$$

and

$$z_s = \frac{-[1 + \Sigma z_o^{-1/3} + Fz_o^{2/3}]}{2(1-\Lambda_s)} \qquad (\delta_s = \zeta = 0) \tag{66}$$

The equilibrium phase compositions are approximated by:

$$\Gamma_\alpha \approx -1 - \frac{\Lambda_s \Gamma_o}{(1-\Lambda_s)} - 2z_s\tau \qquad (\delta_s = \zeta = 0) \tag{67}$$

and

$$\Gamma_\beta \approx 1 - \frac{\Lambda_s \Gamma_o}{(1-\Lambda_s)} - 2z_s\tau \qquad (\delta_s = \zeta = 0) \tag{68}$$

The equilibrium phase fraction and compositions are functions of the alloy composition.

5. RESULTS AND DISCUSSION

When interfacial stresses and Curvatures are neglected, the equations of state for the thin-film and spherical geometries are qualitatively very similar: Both are cubic polynomials in the phase fraction that are functions of the alloy composition (Γ_o), difference in elastic constants (δ_s or δ_p), the scaled stress parameter (Λ_p or Λ_s), and the difference in the curvatures of the free energy of each phase (ζ). When stresses vanish, $\Lambda = 0$, the equilibrium phase fraction for both system geometries is given by the lever rule: $z = (\Gamma_o + 1)/2$. In this case, the phase compositions are constant and independent of the alloy composition (Γ_o). When the scaled stress parameter is nonzero, $\Lambda \neq 0$, the degree of the polynomial equation of state for both geometries depends on the difference in the curvatures of the free energy densities (ζ) and the elastic inhomogeneity (δ). If $\zeta = \delta = 0$, the equation of state in the absence of capillarity is linear in z;[2] while if $\delta = 0$, the equation of state is quadratic in z.[6, 9]

Each root of the cubic polynomial equation of state found in the absence of capillarity and interfacial effects corresponds to a state of the system for which the equilibrium conditions are satisfied. The systems are physical so long as the phase fraction satisfies $0 \leqslant z \leqslant 1$. The bounds $z = 0$ and $z = 1$ correspond to systems comprised entirely of α or β, respectively. These bounds are treated as end-of-range extrema. The equilibrium states can be either stable or unstable with respect to small changes in the phase fraction. We showed previously that for a given temperature, alloy composition, and applied stress, more than one physically realizable equilibrium state can exist.[6]

In the following, we explore the effect of capillarity and interfacial stresses on these equilibrium states. In order to obtain estimates on the shifts in equilibrium phase fraction, we employ the following approximations:

$\rho_o f^{\alpha}_{cc} = 5 \times 10^{10}$ ergs/cm^3; $(C^{\beta}_o - C^{\alpha}_o) = 0.1$; and $Y_{\alpha} = K^{\alpha} \approx 10^{12}$ ergs/cm^3. The magnitude of the interfacial and surface stresses are taken to be $|\hat{f}_I| < 10^3$ dynes/cm and $|\hat{f}_s| < 10^4$ dynes/cm, respectively.[27] Misfit strains are assumed to be on the order of $10^{-3} - 10^{-2}$ and we use $10^{-6} < L < 10^{-2}$ cm. As noted by Cahn and Larché,[2] the scaled stress parameter Λ can achieve values greater than one in the vicinity of a congruent point, see also ref. 10. These effects, which can give rise to such features as a William's point, are not considered here.

5.1. Thin Films

The interfacial curvature vanishes for the thin-film system and the interfacial stress manifests itself as a mechanical boundary condition along the edge of the film. When the misfit strain also vanishes, the equilibrium phase fraction of β is given by solution to Eq. (29). The change in phase fraction from the unstressed value, $(\Gamma_o + 1)/2$, owing to the interfacial stress $\hat{f}_I$ is approximated by Eq. (32) and depends on the magnitude of the parameter Λ_m. Using Eq. (30) and the materials parameters given above, we estimate $\Lambda_m < 10^{-2}$. From the approximation Eq. (32), the shift in phase fraction induced by the interfacial stress depends on the product $\delta_p \Lambda_m$. Thus, within the imposed bounds on the materials parameters, we estimate the effect of interfacial stress on phase fraction to be small, on the order of 1% or less, in the absence of a misfit strain.

The shift in equilibrium phase fraction for a misfit-free alloy owing to the interfacial stress is shown schematically as a function of alloy composition Γ_o on the phase stability diagram of Fig. 3. Solid lines represent equilibrium states that are stable with respect to small changes in z, while dashed lines represent unstable solutions. Three values for the difference in elastic constants, δ_p, are shown. When $\delta_p = 0$, there are no interfacial stress effects and the equilibrium phase fraction and compositions are identical to those of unstressed systems. This is to be expected as the elastic energy density induced by the interfacial stress is the same for both phases and, therefore, does not change the relative stability of one phase with respect to the other. When $\delta_p > 0$, α is the elastically soft phase and the increase in the elastic energy density is greater in the β phase; thereby stabilizing α with respect to β. This results in a shift of the two-phase equilibrium curve to greater alloy compositions. When $\delta_p < 0$, the opposite obtains and the elastically soft β-phase is stabilized with respect to α.

Using the materials parameters given above, $\Lambda_p < 0.4$. From the approximation of Eq. (39) for which the interfacial stress is ignored (nondimensional $\tau^o_{11} = 0$), it is seen that the misfit strain can induce significant changes in the equilibrium phase fraction and phase compositions. Indeed,

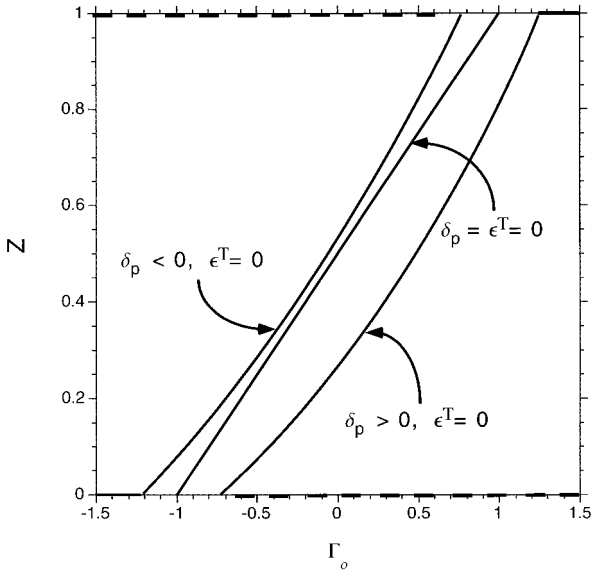

Fig. 3. Phase stability diagram for a misfit-free thin film showing the phase fraction z as a function of reduced alloy composition Γ_o. For an elastically homogeneous system, $\delta_p = 0$, the interfacial stress does not affect the equilibrium state and the equilibrium phase fractions and compositions are identical to those of a stress-free system for all film thicknesses L. If $\delta_p < 0$, the α-phase is harder than the β-phase and the β phase is stabilized by the interfacial stress. If $\delta_p > 0$ the β-phase is the harder phase, and α phase is stabilized.

under the appropriate conditions, the misfit strain can destabilize a two-phase system.[2, 6]

The added effect of the interfacial stress on phase equilibrium can be assessed using the approximation, Eq. (46), for the simple case $\delta_p = 0$ and $\zeta = 0$. The magnitude of the additional shift in phase fraction owing to interfacial stress is determined by the product $\Lambda_p \tau_{11}^o$. For the given set of materials parameters, $\Lambda_p \tau_{11}^o < 0.4$. This indicates that the interfacial stress can exert a significant influence on the system's equilibrium state via an interaction with the misfit strain.

Figure 4 is a phase stability diagram showing the equilibrium phase fraction of β as a function of scaled alloy composition Γ_o. The dotted line spanning $-1 \leqslant \Gamma_o \leqslant 1$ gives the equilibrium phase fraction in the absence of all stress effects ($\Lambda_p = 0$). The three solid lines correspond to stable phase fractions for the case when $\Lambda_p = 0.25$ with different values of τ_{11}^o. When $\hat{f}_I = \tau_{11}^o = 0$ (or the phases are thick), the span of the two-phase field is reduced to alloy compositions $-3/4 < \Gamma_o < 3/4$; the elastic energy of the two-phase system arising from the misfit strain stabilizes a single-phase

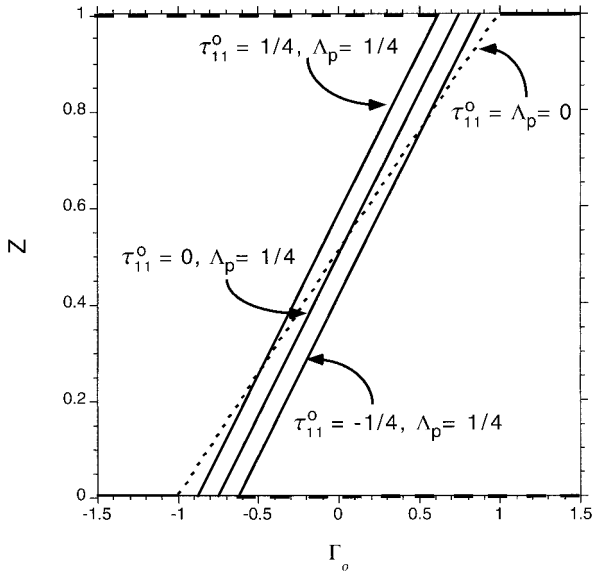

Fig. 4. Phase stability diagram for a thin film showing the phase fraction z as a function of reduced alloy composition Γ_o. The misfit strain (Λ_p) alters the equilibrium phase fraction with respect to the stress-free case (dotted line). Changes in the thickness of the film, L, yield changes in τ^o_{11} that result in further changes in the phase fraction.

system with respect to the two-phase system. The relative stability of the two phases is further affected by the interfacial stress depending on the sign of $\hat{f}_I/\varepsilon$. Figure 4 shows this change in stability for the two cases $\tau^o_{11} = 1/4$ and $\tau^o_{11} = -1/4$. When $\hat{f}_I/\varepsilon < 0$, $\tau^o_{11} > 0$, and β is stabilized with respect to α. This is shown as a shift to the left of the phase fraction in Fig. 4. The phase fraction shifts to the right in Fig. 4 when $\hat{f}_I/\varepsilon > 0$ or $\tau^o_{11} < 0$.

Consider the case when $\hat{f}_I > 0$ and the misfit strain $\varepsilon < 0$. The lattice parameter of stress-free β is less than that of stress-free α so that, in the absence of an interfacial stress, the β-phase is in tension and the α phase is in compression. The positive interfacial stress acts to decrease the lattice parameters of both phases. Since the α-phase is already in compression, the additional compressive force-will increase the elastic energy density in the α-phase while decreasing it in the β-phase; thereby stabilizing the β-phase with respect to the α-phase. Should $\varepsilon > 0$ with $\hat{f}_I > 0$, the interfacial stress will decrease the elastic energy density of α and increase that of β, leading to a stabilization of α with respect to β.

The scaled equilibrium phase compositions, Γ_α and Γ_β are shown as a function of scaled alloy composition Γ_o in Fig. 5. The solid lines depict the phase compositions in the absence of all stress effects. For $\Gamma_o < -1$ and

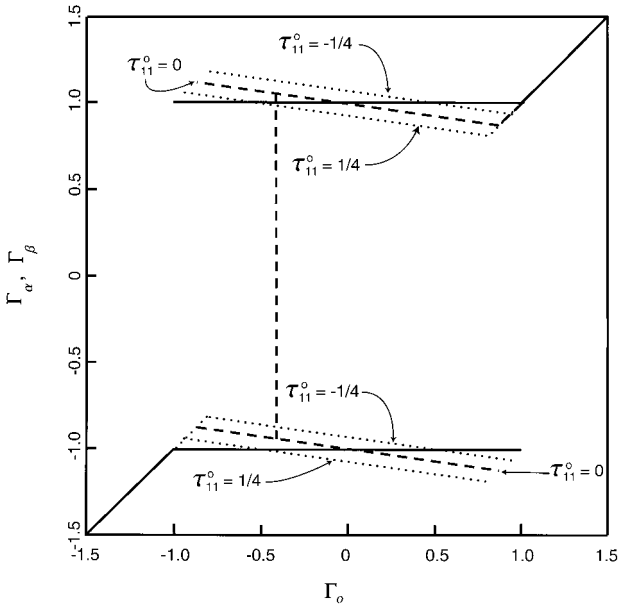

Fig. 5. Scaled compositions of the α phase (Γ_α) and β-phase (Γ_β) are shown as a function of the bulk alloy composition (Γ_o) for the thin film geometry. The β-phase composition is given by the upper curve ($\Gamma_\beta > 0$) and the α-phase composition is given by the lower curve ($\Gamma_\alpha < 0$). The horizontal solid line gives the phase composition in the stress-free case.

$\Gamma_o > 1$, the system is single-phase α and single-phase β, respectively. The equilibrium phase compositions are independent of alloy composition in the stress-free, two-phase state. The dashed line gives the phase compositions for the case $\Lambda_p = 1/4$ and $\tau^o_{11} = 0$. As seen from the phase stability diagram, the two-phase field has been reduced in extent to $-3/4 < \Gamma_o < 3/4$ and, unlike the stress-free situation, the phase compositions are a function of alloy composition. The dotted lines show how the interfacial stress alters the phase compositions for $\tau^o_{11} = 1/4$ and $\tau^o_{11} = -1/4$ when $\Lambda_p = 1/4$.

The change in phase composition induced by the interfacial stress depends on the sign of τ^o_{11} and, hence, on the sign of $\hat{f}_I/\varepsilon$. When $\tau^o_{11} < 0$ ($\hat{f}_I/\varepsilon > 0$), the composition of α is increased, or shifted towards component B, while the β-phase becomes less rich in component B. This is a result of the change in relative stability induced by the interfacial stress. When $\hat{f}_I/\varepsilon > 0$, α is stabilized with respect to β. The system responds to this change in stability by decreasing the phase fraction of β. Mass is conserved in the closed system and the composition of both phases must change. Since β is the solute-rich phase in this case and the phase fraction of β is decreasing, the compositions of each phase must increase. At equilibrium,

the increase in free energy owing to the composition shift is compensated by the decrease in free energy owing to the change in phase fraction. The vertical line in Fig. 5 gives the difference in composition between the two-phases for a given alloy composition. This difference in phase composition remains constant across the two-phase field so long as both $\zeta = 0$ and $\delta_p = 0$. When $\zeta \neq 0$, the change in free energy resulting from a change in composition will be different for each phase.

It is useful to define a nondimensional stress as $\tau_{ij} = T_{ij}/\varepsilon Y_\alpha$. For the thin-film system, the only nonzero stress components are the in-plane stresses $T_{11} = T_{22}$. Substituting the equilibrium phase fraction for the case $\delta_p = \zeta = 0$, Eq. (46), into the expressions for the stress field in Appendix I yields:

$$\tau_{11}^{\alpha} = \frac{1}{2} + \frac{(\Gamma_o + 2\tau_{11}^o)}{2(1 - \Lambda_p)} \tag{69}$$

and

$$\tau_{11}^{\beta} = -\frac{1}{2} + \frac{(\Gamma_o + 2\tau_{11}^o)}{2(1 - \Lambda_p)} \tag{70}$$

The nondimensional force balance on the edge of the film, Eq. (74), becomes:

$$\tau_{11}^o = (1 - z)\,\tau_{11}^{\alpha} + z\tau_{11}^{\beta} \tag{71}$$

Figure 6 gives an example of a stress-composition ($\tau_{11} - \Gamma$) phase diagram calculated with $\Lambda_p = 1/2$. Such a diagram is possible for the thin plate geometry because the equilibrium stresses and compositions are uniform throughout the phases. The solid lines denote field lines, or the limits of the two-phase field. The α-phase line corresponds to $z = 0$ and the β-phase line to $z = 1$. Between these two field lines, two-phase coexistence ($\alpha + \beta$) is possible.

Figure 6 is used much like an isothermal section of a compositional ternary phase diagram.[9] For example, assume the scaled, bulk alloy composition is taken as $\Gamma_o = 0$ and the nondimensional, in-plane applied stress is $\tau_{11}^o = 0$. This latter condition corresponds, for example, to a system in which no external stress is applied ($T_{ap} = 0$) and the film thickness L is very large (the limit for which interfacial stress does not influence equilibrium.) The point ($\Gamma_o = 0$, $\tau_{11}^o = 0$) is indicated on the phase diagram by the open square. The dashed line passing through this point is the tie line, which must be determined from the equilibrium conditions: Eqs. (69) and (70) for the stresses and Eqs. (47 and (48) for the compositions. The intersection of

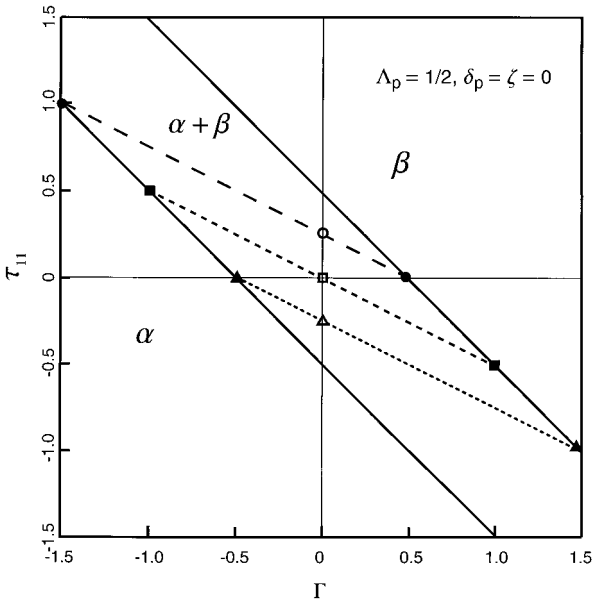

Fig. 6. Diagram showing a region in scaled stress, τ_{11}, and composition Γ-space where a two-phase field exists. The tie lines are dashed and end on the (solid) field lines. The equilibrium phase compositions and in-plane stresses can be read from the ends of the tie lines (filled characters).

the tie line with the α field line gives the equilibrium state of stress and composition of the α phase ($\tau_{11}^{\alpha} = 0.5$, $\Gamma_{\alpha} = -1$). Likewise, the intersection of the tie line with the β field line gives the equilibrium state of stress and composition of the β phase ($\tau_{11}^{\beta} = -0.5$, $\Gamma_{\beta} = 1$). If the alloy composition (Γ_o) and effective applied stress (τ_{11}^{o}) are changed so that their position when plotted on the stress-composition phase diagram remains on this tie line, the equilibrium phase compositions and stresses remain the same, although the volume fraction of the phases will change.

The open circle and triangle depict how the equilibrium phase compositions and stresses will change when the dimension of the planar film is changed (thereby changing τ_{11}^{o}), assuming there is no applied stress ($T_{ap} = 0$) and holding the bulk alloy composition at $\Gamma_o = 0$. As seen from Eq. (36), the sign of the effective stress τ_{11}^{o} depends on the sign of $\hat{f}_I/\varepsilon$ when $T_{ap} = 0$. If $\hat{f}_I/\varepsilon > 0$, then $\tau_{11}^{o} < 0$. If $\tau_{11}^{o} = -0.25$ and $\Gamma_o = 0$, the filled triangles give the equilibrium scaled stresses and compositions of the two phases: $\tau_{11}^{\alpha} = 0$, $\Gamma_{\alpha} = -0.5$ and $\tau_{11}^{\beta} = -1$, $\Gamma_{\beta} = 1.5$. The filled circles give the equilibrium phase compositions and stresses for any effective stress (τ_{11}^{o})

and alloy composition (Γ_o) which lies on the dotted tie line, for example $\tau_{11}^o = 0.25$, $\Gamma_o = 0$.

As the dimensions of the planar system decreases, the magnitude of τ_{11}^o increases, the direction of which is determined by the sign of $\hat{f}_I/\varepsilon$. Depending upon the bulk alloy composition, it is possible for the interfacial stress to stabilize a single-phase field in what would otherwise be a two-phase field. The slopes of the field and tie lines are determined from the equilibrium conditions and will depend on the magnitude of Λ_p.

5.2. Concentric Spheres

The sphere dimension affects the equilibrium phase fraction and compositions directly through the surface stress term and indirectly through the interfacial stress and interfacial energies The magnitude of these effects to first-order in τ (the reciprocal of the outer sphere radius) can be estimated using Eqs. (64)–(68). As defined by Eq. (59), τ can be either positive or negative depending on the sign of $\varepsilon\hat{f}_s$. For illustrative purposes, we assume a positive misfit strain in β and a tensile surface stress so that $\varepsilon\hat{f}_s > 0$ and $\tau > 0$. As seen from Eqs. (64) and (66), the α-phase is stabilized with respect to β when $\tau > 0$. For example, when both $\hat{f}_s$ and ε are positive, the compressive stresses engendered by the tensile surface stress makes the α-phase, with its smaller lattice parameter, more stable than the β-phase, and there is a shift in the equilibrium phase fraction to a smaller value of z. Using the approximate materials parameters given previously, using Eq. (66) we find that particles with radii on the order of 50–100 nm could induce a shift in the equilibrium phase fraction on the order of 0.1.

The nondimensional interfacial term Σ and F also appear in Eq. (66). As both Σ and F can be either positive or negative they can act to stabilize either of the phases. In most instances, we expect $|F| < 1$, as usually $|\hat{f}_I| < |\hat{f}_s|$. However, for coherent systems, it seems likely that $|\Sigma| \approx O(1)$.

The interfacial stress and interfacial energy represent independent means of creating new interfacial area, the former by moving atoms from the bulk to the interface and the latter by stretching the interface. As a result, the interfacial energy can be a function of the stress state of the bulk phases at the interface through the presence of a nonzero interfacial stress. In the planar geometry, this dependence has no effect on the equilibrium conditions, due to the planarity of the interfaces. In contrast, in the concentric sphere case, the dependence of the interfacial energy on the interfacial stress affects the equilibrium state of the system. Moreover, this coupling to the bulk stresses introduces a dependence of the interfacial energy on the volume fraction of the phases. Thus, not only do the bulk phase compositions depend on the volume fraction in elastically stressed solids, but the the interfacial energy does as well.

A major difference between the concentric sphere and thin-film geometries is the uniformity of the stress fields in the two phases; the stress field in the concentric sphere case is position-dependent within a phase, whereas the stress field in the planar geometry is uniform throughout a phase. This difference in the spatial dependence of the stress field could result in qualitatively different behavior of the phase equilibria. For example, in the thin-film case, a classical phase rule can be shown to exist,[9] whereas in the concentric sphere case it is not clear if a phase rule exists.[6, 7, 18] In addition, as was illustrated in Fig. 6, the in-plane stress components in the planar geometry are thermodynamic densities and can be controlled experimentally through the applied stress. This is not possible in the spherical system with a spatially varying stress. The difference in the behavior of these two systems illustrates the rich behavior that is possible in elastically stressed systems.

6. SUMMARY

We have shown that interfacial and surface stresses can affect the equilibrium phase fraction and composition in two-phase binary alloys, as compared to large unstressed systems, when one or more of the system's physical dimensions becomes small. The nature of this effect was explored for two system-geometries that guarantee equilibrium, concentric spheres and planar thin films. In both cases, the magnitude of the shift in the equilibrium phase fraction and compositions from the unstressed values depends on various thermodynamic and materials parameters, as well as the system size and geometry. The equations of state for both systems have been examined only in the limit of small changes in phase composition, and a full nonlinear treatment of the problem remains to be performed.

In the thin-film or planar geometry, the interfacial stress acts in a manner similiar to that of an applied stress in the plane of the film and with a magnitude proportional to the reciprocal film thickness. The thermodynamic state of each phase remains spatially uniform and it is possible to construct a stress-composition phase diagram that shows the effect of film thickness on the equilibrium compositions and stresses within the phases. The interfacial stress effect is strongest when there is a misfit between the phases and the system is elastically inhomogeneous

For the case of two concentric spheres, the presence of an interfacial stress leads to a dependence of both the elastic energy and the interfacial energy on the phase fraction. In addition, the surface stress will affect the relative stability of the phases and their equilibrium compositions, through its interaction with the misfit strain and different elastic constants of the phases; we estimate that shifts in phase fraction on the order of 0.1 might be possible for spheres with radii as large as 50–100 nm.

APPENDIX I

In this appendix, the elastic stresses and strains associated with the thin-film geometry are calculated using the mechanical equilibrium conditions. Owing to the stacking of the thin films (plates), bending in the system is prohibited, and the elastic state within each phase is uniform. Invoking the coherency condition at the $\alpha-\beta$ interface, Eq. (3), further requires the strains in the plane of the interface to be equal. Since no stress is applied in the x_3 direction and the interface remains planar, the normal stress in each phase must vanish according to the traction condition of Eq. (4). This gives:

$$E_{11}^{\alpha} = E_{22}^{\alpha} = E_{11}^{\beta} = E_{22}^{\beta} \qquad \text{and} \qquad T_{33}^{\alpha} = T_{33}^{\beta} = 0 \tag{72}$$

A mechanical force balance along the edge of the plates can be obtained by considering one unit of the array:

$$l_{\alpha} w T_{11}^{\alpha} + l_{\beta} w T_{11}^{\beta} + 2w\hat{f}_I = wLT_{ap} \tag{73}$$

where T_{ap} is the stress applied along the edge of the film, w is the width of the film, and l_{α} and l_{β} are the thickness of the α and β phase lyers, respectively (Fig. 1). If $L = l_{\alpha} + l_{\beta}$ is the periodicity of the layers, $z = l_{\beta}/L$ is the phase fraction of the β-phase, and the force balance of Eq. (73) becomes:

$$(1-z)\, T_{11}^{\alpha} + zT_{11}^{\beta} = T_{ap} - 2\hat{f}_I/L = T_{11}^{o} \tag{74}$$

where T_{11}^{o} is the effective, in-plane stress for the system. The Voigt elastic constants for a cubic crystal, C_{11}, C_{12} and C_{44} can be used to express the stresses in terms of the strain components with Eq. (1). Substituting these expressions into the force balance, Eq. (74), and solving for the strain E_{11} yields:

$$E_{11} = E_{22}^{\alpha} = E_{11}^{\beta} = E_{22}^{\beta} = \frac{T_{ap} - 2\hat{f}_I/L + Y_{\beta}\varepsilon z}{Y_{\alpha} + (Y_{\beta} - Y_{\alpha})\, z} \tag{75}$$

with

$$E_{33}^{\alpha} = -2C_{12}^{\alpha} E_{11}/C_{11}^{\alpha} \qquad \text{and} \qquad E_{33}^{\beta} = -2C_{12}^{\beta} E_{11}/C_{11}^{\beta} \tag{76}$$

where the planar elastic modulus Y is defined for each phase as:

$$Y = (C_{11} - C_{12})(C_{11} + 2C_{12})/C_{11} \tag{77}$$

The stresses in each phase are:

$$T_{11}^{\alpha} = T_{22}^{\alpha} = Y_{\alpha} E_{11} \qquad \text{and} \qquad T_{11}^{\beta} = T_{22}^{\beta} = Y_{\beta}(E_{11} - \varepsilon) \tag{78}$$

The strain energy densities are:

$$\tfrac{1}{2} T^{\alpha}_{ij} E^{\alpha}_{ij} = Y_{\alpha} E^{2}_{11} \tag{79}$$

and

$$\tfrac{1}{2} T^{\beta}_{ij} (E^{\beta}_{ij} - E^{T}_{ij}) = Y_{\beta} (E_{11} - \varepsilon)^2 \tag{80}$$

APPENDIX II

The elastic field associated with the concentric sphere model is obtained using spherical coordinates and isotropic elasticity. Let u_r be the radial displacement component. Spherical symmetry then requires:[26]

$$u^{\beta}_{r} = B_1 r \qquad \text{and} \qquad u^{\alpha}_{r} = B_2 r + B_3/r^2 \tag{81}$$

where r is the radial position coordinate, and B_1, B_2 and B_3 are constants to be determined from the boundary conditions. The elastic field determined by the displacements in Eq. (81) satisfy the mechanical equilibrium conditions of Eq. (2). The non-zero strain components obtained from the displacement fields are:

$$E^{\beta}_{rr} = E^{\beta}_{\theta\theta} = E^{\beta}_{\phi\phi} = B_1 \tag{82}$$

$$E^{\alpha}_{rr} = B_2 - 2B_3/r^3 \qquad \text{and} \qquad E^{\alpha}_{\theta\theta} = E^{\alpha}_{\phi\phi} = B_2 + B_3/r^3 \tag{83}$$

The corresponding stresses are:

$$T^{\beta}_{rr} = T^{\beta}_{\theta\theta} = T^{\beta}_{\phi\phi} = 3K^{\beta}(B_1 - \varepsilon) \tag{84}$$

and

$$T^{\alpha}_{rr} = 3K^{\alpha}B_2 - 4\mu^{\alpha}B_3/r^3 \qquad \text{and} \qquad T^{\alpha}_{\theta\theta} = T^{\alpha}_{\phi\phi} = 3K^{\alpha}B_2 + 2\mu^{\alpha}B_3/r^3 \tag{85}$$

where K and μ are the bulk modulus and shear modulus, respectively, of the indicated phase.

The three unknown coefficients are obtained from the coherency constraint at the $\alpha - \beta$ interface and the two mechanical force balances. The coherency constraint, Eq. (3), gives $u^{\alpha}_{r}(R^{\beta}) = u^{\beta}_{r}(R^{\beta})$ or:

$$B_2 R^{\beta} + B_3/(R^{\beta})^2 = B_1 R^{\beta} \tag{86}$$

The mechanical force balance at the $\alpha - \beta$ interface, Eq. (4), becomes:

$$T^{\beta}_{rr} = T^{\alpha}_{rr} - \kappa^{\beta}\hat{f}_I \qquad \text{or} \qquad 3K^{\beta}(B_1 - \varepsilon) = 3B_2K^{\alpha} - 4\mu^{\alpha}B_3/(R^{\beta})^3 - 2\hat{f}_I/R^{\beta} \tag{87}$$

The mechanical force balance at the outer surface requires:

$$T^{\alpha}_{rr} = 3B_2K^{\alpha} - 4\mu^{\alpha}B_3/(R^{\alpha})^3 = -(P_{ext} + 2\hat{f}_s/R^{\alpha}) \tag{88}$$

Defining:

$$P = (P_{ext} + 2\hat{f}_s/R^{\alpha})/3K^{\alpha} \tag{89}$$

and

$$e = \varepsilon - \frac{2\hat{f}_I}{3K^{\beta}R^{\beta}} \tag{90}$$

and solving the above equations for the B_i yields the following expressions for the stress and strain fields:

$$E^{\beta}_{rr} = E^{\beta}_{\theta\theta} = E^{\beta}_{\phi\phi} = A + 3K^{\alpha}(A + P)/4\mu^{\alpha}z \tag{91}$$

$$E^{\alpha}_{rr} = A - 3K^{\alpha}(R^{\alpha})^3\,(A + P)/2\mu^{\alpha}r^3 \tag{92}$$

$$E^{\alpha}_{\theta\theta} = E^{\alpha}_{\phi\phi} = A + 3K^{\alpha}(R^{\alpha})^3\,(A + P)/4\mu^{\alpha}r^3 \tag{93}$$

$$T^{\beta}_{rr} = T^{\beta}_{\theta\theta} = T^{\beta}_{\phi\phi} = 3K^{\beta}(E^{\beta}_{rr} - \varepsilon) \tag{94}$$

$$T^{\alpha}_{rr} = 3K^{\alpha}A - 3K^{\alpha}(R^{\alpha})^3\,(A + P)/r^3 \tag{95}$$

$$T^{\alpha}_{\theta\theta} = T^{\alpha}_{\phi\phi} = 3K^{\alpha}A + 3K^{\alpha}(R^{\alpha})^3\,(A + P)/2r^3 \tag{96}$$

where:

$$A = \frac{12\mu^{\alpha}K^{\beta}ez - 3K^{\alpha}(3K^{\beta} + 4\mu^{\alpha})\,P}{3K^{\alpha}(3K^{\beta} + 4\mu^{\alpha}) + 12\mu^{\alpha}(K^{\beta} - K^{\alpha})\,z} \tag{97}$$

APPENDIX III

For a stress-free binary alloy, the diffusion potential, or the difference in chemical potentials between species, is equal to the first derivative with respect to composition (C) of the Helmholtz free energy per atom, f:

$$M_{BA}(C) = \mu_B(C) - \mu_A(C) = \frac{\partial f}{\partial C} = f_c \tag{98}$$

Expanding the diffusion potential about the respective, stress-free equilibrium phase composition yields,

$$M_{BA}(C) = M_{BA}(C_o) + f_{cc}(C - C_o) + O((C - C_o)^2) \tag{99}$$

for both phases. Since in the stress-free state, $M^{\alpha}_{BA}(C^{\alpha}_o) = M^{\beta}_{BA}(C^{\beta}_o)$, using Eq. (7) we obtain Eq. (14).

ACKNOWLEDGMENTS

We would like to thank P. H. Leo for many helpful discussions. We gratefully acknowledge the support of the Division of Materials Research, National Science Foundation under grant DMR-9496133 (WCJ) and DMR-9707073 (PWV).

REFERENCES

1. J. W. Cahn, *Acta Metall.* **10**:907 (1962).
2. J. W. Cahn and F. C. Larché, *Acta Metall.* **32**:1915 (1984).
3. R. O. Williams, *Metall. Trans.* **9A**:1353 (1978).
4. J. W. Cahn, *Acta Metall.* **28**:1333 (1980).
5. J. W. Cahn and F. C. Larché, *Acta Metall.* **30**:51 (1982).
6. W. C. Johnson and P. W. Voorhees, *Metall. Trans.* **18A**:1213 (1987).
7. W. C. Johnson, *Metall. Trans.* **18A**:1093 (1987).
8. M. J. Pfeiffer and P.W. Voorhees, *Acta Metall. Mater.* **39**:2001 (1991).
9. W. C. Johnson and W. H. Müller, *Acta Metall. Mater.* **39**:89 (1991).
10. M. J. Pfeiffer and P. W. Voorhees, *Metall. Trans. A* **22**:1921 (1991).
11. M. J. Pfeiffer and P. W. Voorhees, *Scripta Metall. et Mater.* **30**:743 (1994).
12. D. K. Na, J. B. Cohen, and P. W. Voorhees, *Scripta Metall. et Mater.* **35**:597 (1996).
13. J. Y. Huh and W. C. Johnson, *Acta Metall. Mater.* **43**:1631 (1995).
14. P.-Y. F. Robin, in *Proc. Int. Conf. Solid-solid Phase Transform.* H. I. Aaronson, D. E. Laughlin, R. F. Sekerka, and M. Wayman, eds., TMS-AIME, 1011 (1982).
15. Z. K. Liu and J. Ågren, *Acta Metall. Mater.* **38**:561 (1990).
16. J. K. Lee and W. M. Tao, *Acta Metall. Mater.* **42**:569 (1994).
17. A. L. Roytburd and J. Slutsker, *J. Appl. Phys.* **77**:2745 (1995).
18. Z. K. Liu and J. Ågren, *J. Phase Equil.* **16**:30 (1995).
19. A. J. Ardell and A. Maheshwari, *Acta Metall. et Mater.* **43**:1825 (1995).
20. R. B. Schwarz and A. G. Khachaturyan, *Phys. Rev. Lett.* **74**:2523 (1995).
21. P. W. Voorhees and W. C. Johnson, *J. Chem. Phys.* **84**:5108 (1986).
22. W. A. Jesser, *Mats. Sci. Engr.* **4**:279 (1969).
23. F. C. Larché and J. W. Cahn, *Acta Metall.* **21**:1051 (1973).
24. F. C. Larché and J. W. Cahn, *Acta Metall.* **26**:53 (1978).
25. P. H. Leo and R. F. Sekerka, *Acta Metall.* **37** (1989).
26. L. E. Malvern, *Introduction to the Mechanics of a Continuous Medium* (Prentice-Hall, New Jersey, 1969).
27. R. A. Johnson, *Surf. Sci.* **335**:241 (1996).